

Mechanism of the Six-Electron Reduction of Nitrite to Ammonia by Cytochrome *c* Nitrite Reductase

Oliver Einsle,^{*,†,‡} Albrecht Messerschmidt,[†] Robert Huber,[†]
Peter M. H. Kroneck,[§] and Frank Neese^{*,§,||}

Contribution from the Max-Planck-Institut für Biochemie, Abt. Strukturforchung,
Am Klopferspitz 18a, 82152 Martinsried, Germany, and Universität Konstanz,
Mathematisch-Naturwissenschaftliche Sektion, Fachbereich Biologie, Universitätsstrasse 10,
78457 Konstanz, Germany

Received May 6, 2002

Abstract: Cytochrome *c* nitrite reductase catalyzes the six-electron reduction of nitrite to ammonia without the release of potential reaction intermediates, such as NO or hydroxylamine. On the basis of the crystallographic observation of reaction intermediates and of density functional calculations, we present a working hypothesis for the reaction mechanism of this multiheme enzyme which carries a novel lysine-coordinated heme group (Fe-Lys). It is proposed that nitrite reduction starts with a heterolytic cleavage of the N–O bond which is facilitated by a pronounced back-bonding interaction of nitrite coordinated through nitrogen to the reduced (Fe(II)) but not the oxidized (Fe(III)) active site iron. This step leads to the formation of an {FeNO}⁶ species and a water molecule and is further facilitated by a hydrogen bonding network that induces an electronic asymmetry in the nitrite molecule that weakens one N–O bond and strengthens the other. Subsequently, two rapid one-electron reductions lead to an {FeNO}⁸ form and, by protonation, to an Fe(II)–HNO adduct. Hereafter, hydroxylamine will be formed by a consecutive two-electron two-proton step which is dehydrated in the final two-electron reduction step to give ammonia and an additional water molecule. A single electron reduction of the active site closes the catalytic cycle.

Introduction

Although most of the metalloenzymes involved in the fundamental biogeochemical cycles of nitrogen and sulfur have been well characterized and structural information has become available for the majority of them, many important questions remain concerning their reaction mechanisms and modes of operation. Two remarkable steps involve the six-electron reductions of nitrite to ammonia and of sulfite to sulfide. In both cases, there exist assimilatory systems to provide reduced nitrogen or sulfur for biosynthetic purposes as well as dissimilatory systems which serve in energy conservation.^{1,2} The assimilatory enzymes and dissimilatory sulfite reductase contain a siroheme moiety, a bacterioisochlorin linked via cysteine to a [4Fe4S] cluster.³ In contrast to this, dissimilatory cytochrome *c* nitrite reductase (ccNiR) is a multiheme *c* enzyme, and its active site is a protoporphyrin IX which is covalently linked to

the protein backbone. A lysine was found to replace the usual histidine as a proximal ligand to the heme iron.⁴ This enzyme catalyzes the reduction of both nitrite and sulfite with high specific activity and obtains electrons from the membrane-associated quinone pool, thereby generating a proton motive force.⁴

Having solved the X-ray structures of ccNiR from *Sulfurospirillum deleyianum*⁴ and *Wolinella succinogenes*,⁵ we raised the question as to how substrate reduction is actually achieved. We have, therefore, structurally characterized complexes of the *W. succinogenes* enzyme with nitrite and with the putative reaction intermediate hydroxylamine. The reaction of ccNiR starts with the binding of nitrite, and ammonia is produced without the release of intermediates such as NO or hydroxylamine. Both NO and hydroxylamine were reduced to ammonia by ccNiR, with specific activities of ~50% for hydroxylamine but of only ~1.2% for nitric oxide relative to the one for nitrite.⁶

Earlier, the three-dimensional structure of the *W. succinogenes* ccNiR had been characterized, with all heme centers in the Fe(III) state and a water molecule coordinated to the Fe-Lys active site.⁵ In the present work, we used a combination of crystallographic analyses of substrate complexes (Figure 1A, 3) and density functional calculations for a simplified model system

* Correspondence should be addressed to O.E. (einsle@caltech.edu) or F.N. (neese@mpi-muelheim.mpg.de).

† Max-Planck-Institut für Biochemie.

‡ Present address: Howard Hughes Medical Institute and Division of Chemistry and Chemical Engineering, California Institute of Technology, mail code 147-75CH, Pasadena, California 91125, USA. Telephone: +1 (626) 395-8392. Fax: +1 (626) 584-6785.

§ Universität Konstanz.

|| Present address: Max-Planck-Institut für Strahlenchemie, Stiftstrasse 34-36, 45470 Mülheim an der Ruhr, Germany.

(1) Cole, J. A.; Brown, C. M. *FEMS Microbiol. Lett.* **1980**, *7*, 65–72.

(2) Berks, B. C.; Richardson, D. J.; Reilly, A.; Willis, A. C.; Ferguson, S. J. *Biochem. J.* **1995**, *309*, 983–992.

(3) Crane, B. R.; Siegel, L. M.; Getzoff, E. D. *Science* **1995**, *270*, 59–67.

(4) Einsle, O.; Messerschmidt, A.; Stach, P.; Bourenkov, G. P.; Bartunik, H. D.; Huber, R.; Kroneck, P. M. H. *Nature* **1999**, *400*, 476–480.

(5) Einsle, O.; Stach, P.; Messerschmidt, A.; Simon, J.; Kröger, A.; Huber, R.; Kroneck, P. M. H. *J. Biol. Chem.* **2000**, *275*, 39608–39616.

(6) Stach, P.; Einsle, O.; Schumacher, W.; Kurun, E.; Kroneck, P. M. H. *J. Inorg. Biochem.* **2000**, *79*, 381–385.

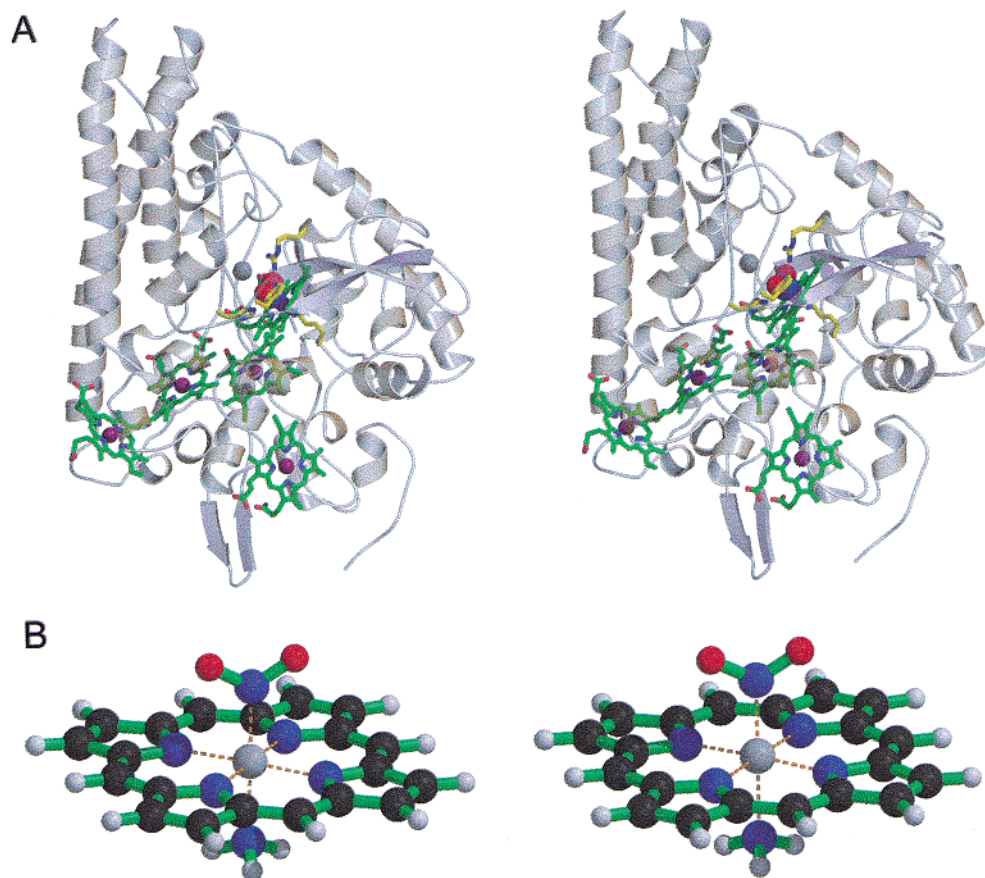


Figure 1. (A) Overall structure of ccNiR. Shown is a monomer with the substrate nitrite bound to the active site. The five heme groups are depicted in green. The proximal lysine ligand at the active site, Lys 133, and the active site residues Arg 114, Tyr 218, and His 277 are shown in yellow; the calcium atom close to the active site is in gray. (B) Simplified active site model used for density functional calculations. An amine nitrogen represents the proximal lysine ligand, and the distal ligand in the model shown is the nitrite anion.

to map out a reaction pathway. For all calculations, an iron–porphyrin with a proximal ammonia nitrogen ligand and various reaction intermediates as distal ligands, $[\text{Fe}(\text{P})(\text{NH}_3)(\text{X})]$, were employed (Figure 1B). While such a system necessarily comes short of taking into account various influences of the surrounding protein, such as electrostatic surface potential and activation of intermediates through binding to protein residues, it provides insight into the dominant electronic structure contributions to the reactivity of the active site metal ion.^{7,8} As an experimental constraint, it is not feasible to solve crystal structures for the reduced forms of the active site, as this would lead to immediate turnover. We have, therefore, followed the strategy to solve the structures in the oxidized (Fe(III)) form of the active site. The comparison of experimental structures for the oxidized protein with the calculated structures then gives confidence that the predictions of the calculations for the reduced (Fe(II)) species are also reasonable.

Materials and Methods

Crystallization and Preparation of Substrate Complexes. NiR was isolated from the membrane fraction of *W. succinogenes* cells.⁹ Triton X-100, which was used during purification, was removed from the protein with a DetergentOUT column (Geno Technologies, St. Louis, MO). Crystals of the protein were grown as described previously⁵

and harvested into a buffer containing 14% poly(ethylene glycol) 4000 and 100 mM sodium acetate/acetic acid, pH 5.7.

Substrate complexes with nitrite were obtained by soaking the crystals with 100 mM sodium nitrite for 1 h before measurement. It was also possible to prepare a nitrite complex by cocrystallization with 25 mM sodium nitrite added to the crystallization buffer. The solution 10% v/v 2*R*,3*R*-butane diol was added to 10% (v/v) as a cryoprotectant immediately prior to cooling the crystals. Data sets were measured on the beamline BW6, DESY, Hamburg, at a wavelength of 1.05 Å. Hydroxylamine proved to be detrimental to the crystals and was used for soaking at a concentration of 5 mM for 15 min. Even so, all data sets measured using synchrotron radiation showed a mixture of species at the active site, probably because of photoreduction caused by the intense radiation. However, data measured with Cu K_{α} radiation yielded a clearly interpretable electron density for the hydroxylamine adduct.

Structure Solution and Refinement. Structures of substrate complexes were phased using the model coordinates of the isomorphous native structure and refined with CNS.¹⁰ Any additional model building was carried out with O.¹¹ Refinement statistics are summarized in Table 1. The electron density maps shown in Figure 2 are $F_o - F_c$ difference electron density maps contoured at 4.5σ , calculated without contribution from the respective substrate molecule.

Calculations. Calculations were done with the TurboMole 5.2 program suite.¹² In the geometry optimizations, the BP86 functional^{13,14}

(7) Solomon, E. I.; Lowery, M. D. *Science* **1993**, 259, 1575.

(8) Siegbahn, P. E. M.; Blomberg, M. R. A. *Chem. Rev.* **2000**, 100, 421–437.

(9) Schumacher, W.; Hole, U.; Kroneck, P. M. H. *Biochem. Biophys. Res. Commun.* **1994**, 205, 911–916.

(10) Brünger, A. T.; Adams, P. D.; Clore, G. M.; Delano, W. L.; Gros, P.; Grosse-Kunstleve, R. W.; Jiang, J. S.; Kuszewski, J.; Nilges, M.; Pannu, N. S.; Read, R. J.; Rice, L. M.; Simonson, T.; Warren, G. L. *Acta Crystallogr., Sect. D* **1998**, 54, 905–921.

(11) Jones, T. A.; Zou, J.-Y.; Cowan, S. W.; Kjeldgaard, M. *Acta Crystallogr., Sect. A* **1991**, 47, 110–119.

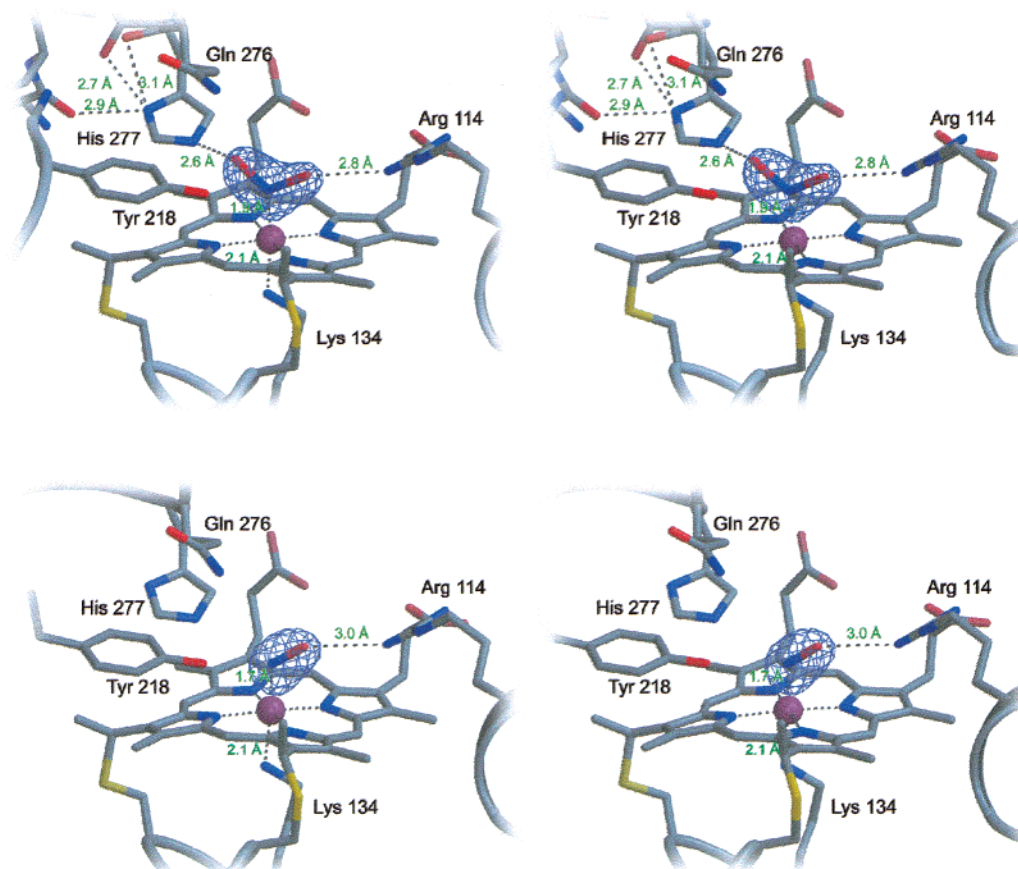


Figure 2. Structures of ccNiR substrate complexes. (A) Nitrite. The substrate binds to the Fe(III) atom of heme 1 through its nitrogen atom, with an observed binding distance of 1.9 Å. Its oxygen atoms are hydrogen bonded to Arg 114 and His 277. Furthermore, the N₃ atom of His 277 takes part in a hydrogen bond network within the protein, which might facilitate deprotonation of the N_e atom of the same imidazole ring. This proton is then used for the immediate formation of water and nitrosyl upon binding of nitrite to the reduced enzyme. (B) Complex of ccNiR with hydroxylamine. The potential reaction intermediate binds to the Fe(III) atom of heme 1 through the nitrogen atom. Its position corresponds exactly to one nitrogen and one oxygen atom of nitrite (Figure 2A).

Table 1. Refinement Statistics for the Substrate and Reaction Intermediate Complexes of Nitrite Reductase

	nitrite	hydroxylamine
unit cell dimensions (a = b, c) (Å)	118.98, 186.73	119.89, 186.22
resolution limits (Å)	50.0–1.60	25.0–2.00
no. of reflections	90 184	45 781
completeness (outer shell) (%)	99.6 (100.0)	99.5 (99.7)
R _{sym} (outer shell)	0.075 (0.420)	0.079 (0.488)
I/σ(I) (outer shell)	18.5 (1.5)	12.8 (2.0)
crystallographic R-factor (R _{free})	0.186 (0.210)	0.189 (0.225)
rmsd in bond lengths	0.005	0.006
rmsd in bond angles	1.184	2.262

was used in conjunction with the SV(P) basis set (a basis set of double- ζ plus polarization quality) for the ligands¹⁵ and with the TZVP basis set (a basis set of valence triple- ζ plus polarization quality) for iron.¹⁶ All geometries have been fully optimized. The final energies were computed at the B3LYP level^{13,17–19} with the program ORCA.²⁰ In these

calculations, the basis set for the iron atom was of all-electron polarized triple- ζ quality,¹⁶ while all other atoms were described with the DZVP basis.²¹ In general, spin-unrestricted calculations were carried out. Structures and energies were computed for various spin states corresponding to high-, intermediate-, and low-spin configurations on the central iron as explained in detail below. Effects of the protein environment and zero-point energies were neglected throughout, and thus, the theoretical study is focused on the primary electronic effects at the active site. The lysine ligand of the active site was modeled by NH₃.

Results and Discussion

In the periplasm of *W. succinogenes*, ccNiR (or NrfA after the name of the encoding gene) forms a stable, membrane-associated complex with its electron donor NrfH, a member of the NapC/NirT family of tetraheme cytochromes, which serves as a quinone oxidase to obtain electrons directly from the membraneous quinone pool.^{22,23} Most likely, this complex consists of a heterotetrameric unit, NrfH₂A₂, with a total of eighteen coupled heme centers which guarantee a fast and

- (12) Ahlrichs, R.; Bär, M.; Baron, H. P.; Bauernschmitt, R.; Böcker, S.; Ehrig, M.; Eichkorn, K.; Elliott, S.; Furche, F.; Haase, F.; Häser, M.; Horn, H.; Huber, C.; Hummer, U.; Kattaneck, M.; Kölmel, C.; Kollwitz, M.; May, K.; Ochsenfeld, C.; Öhm, H.; Schäfer, A.; Schneider, U.; Treutler, O.; von Arnim, M.; Weigend, F.; Weis, P.; Weiss, H. *TurboMole 5.2*; University of Karlsruhe: Karlsruhe, Germany, 2000.
- (13) Becke, A. D. *Phys. Rev. A* **1988**, *38*, 3098.
- (14) Perdew, J. P. *Phys. Rev. B* **1986**, *33*, 8822.
- (15) Schäfer, A.; Horn, H.; Ahlrichs, R. *J. Chem. Phys.* **1992**, *97*, 2571–2577.
- (16) Schäfer, A.; Huber, C.; Ahlrichs, R. *J. Chem. Phys.* **1994**, *100*, 5829.
- (17) Becke, A. D. *J. Chem. Phys.* **1993**, *98*, 1372.
- (18) Becke, A. D. *J. Chem. Phys.* **1993**, *98*, 5648.
- (19) Lee, A. M.; Yang, W.; Parr, R. G. *Phys. Rev. B* **1988**, *37*, 785.

- (20) Neese, F. *ORCA 2.1*, revision 72, may 2001 ed.; Max-Planck-Institut für Strahlenchemie: Mülheim, Germany, 2001.
- (21) Godbout, N.; Salahub, D. R.; Andzelm, J.; Wimmer, E. *Can. J. Chem.* **1992**, *70*, 560–571.
- (22) Simon, J.; Gross, R.; Einsle, O.; Kroneck, P. M. H.; Kröger, A.; Klimmek, O. *Mol. Microbiol.* **2000**, *35*, 686–696.
- (23) Simon, J.; Pisa, R.; Stein, T.; Eichler, R.; Klimmek, O.; Gross, R. *J. Biochem.* **2001**, *268*, 5776–5782.

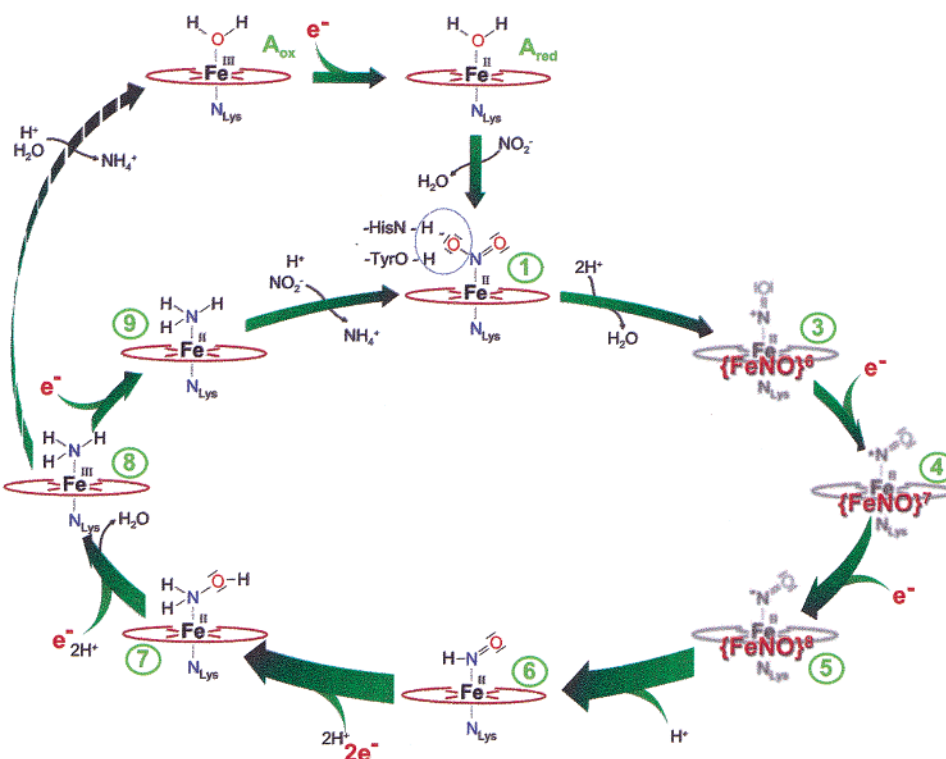


Figure 3. Proposed reaction scheme for ccNiR. When started from the water-bound resting state in either the oxidized or reduced form, the binding of the substrate nitrite starts the reaction cycle, which, after a heterolytic cleavage of the first N–O bond, proceeds through two one-electron reductions and a protonation step to Fe(II)–HNO, which is readily reduced by two electrons to Fe(II)–H₂NOH. A further reduction leads to the dissociation of the second water molecule, and subsequently, after the last reduction step, the product ammonia can dissociate.

Table 2. Summary of the Calculated Bond Lengths for the Proximal and Distal Axial Heme Iron Ligands for Different Adducts

	ferrous (Fe(II))				ΔE^a (kcal/mol)	ferric (Fe(III))				ΔE^a (kcal/mol)
	low-spin		high-spin			low-spin		high-spin		
	R(Fe–X) ^b	R(Fe–NH ₃) ^c	R(Fe–X) ^b	R(Fe–NH ₃) ^c		R(Fe–X) ^b	R(Fe–NH ₃) ^c	R(Fe–X) ^b	R(Fe–NH ₃) ^c	
H ₂ O	2.070	2.000	2.385	2.068	+1.8	1.917	1.973	2.261	2.052	–8.4
OH [–]						1.804	2.016	1.860	2.084	–8.1
NO ₂ [–]	1.932	2.105	2.236	2.371	+15.7	1.922	2.109	2.292	2.292	+7.9
NO	1.772	2.120				1.630	2.034			
NO [–]	1.790	2.271	1.757	2.249	–1.1					
HNO	1.782	2.090	2.003	2.302	+16.3	1.830	2.076	1.830	2.076	+9.4
H ₂ NOH	1.990	2.019	2.275	2.275	+7.8	1.998	2.013	2.278	2.241	+2.0
NH ₃	2.015	2.015	2.280	2.280	+7.25	2.013	2.013	2.253	2.253	+1.3
none				2.191	–7.7				2.164	–12.2

^a $\Delta E = E_{\text{high-spin}} - E_{\text{low-spin}}$. For negative numbers, the high-spin state is lower in energy. ^b R(Fe–X) is the distance (in angstrom) from the iron to the nonprotein sixth ligand. ^c R(Fe–NH₃) is the distance to the axial ammonia ligand that replaces the lysine in the actual structure.

efficient electron transfer to two independent Fe–Lys active sites.⁵ We, therefore, assume that, under physiological conditions, electron transfer to the active site is fast as compared with spatial rearrangements of atoms associated with the breaking and forming of bonds.

Although this implies a reduced active site iron in every step of the reaction, substrate binding could only be investigated crystallographically with all iron centers in the Fe(III) state because of the high activity of ccNiR under reducing conditions. Furthermore, because of the close proximity of the strongly scattering iron atom in the active site, iron–nitrogen bond lengths may be underestimated.²⁴

Combining the structural information obtained for substrate and intermediate complexes with theoretical calculations, we

propose a putative reaction mechanism for ccNiR (Figure 3) which will be discussed step by step in the following.

Substrate Binding. In the crystal structure of the resting Fe(III) form, the distal ligand was modeled as a water molecule (A_{ox}, Figure 3) on the basis of the observed Fe–O bond length of 2.1 Å. This is in agreement with our calculations which show hydroxide ion and water distances to high-spin Fe(III) to be 1.86 and 2.26 Å, respectively (Table 2). For the Fe(II) form, the calculations predict a fairly weakly bound water at a bond length of 2.39 Å and a high-spin (*S* = 2) electronic configuration (A_{red}, Figure 3). Because of the weakness of the Fe(II)–OH₂ bond, it also appears to be possible that water dissociates from the active site after reduction and prior to nitrite binding.

From the resting state, water has to be exchanged for substrate. Interestingly, in the diverse group of nitrite-reducing enzymes, the substrate nitrite is bound through the nitrogen atom

(24) Fülöp, V.; Watmough, N. J.; Ferguson, S. J. *Adv. Inorg. Chem.* **2001**, *51*, 163–204.

to iron in cytochrome *cd*₁²⁵ and in siroheme sulfite reductase²⁶ but through both of the oxygen atoms to Cu in the copper-containing nitrite reductase.²⁷ Thus, we calculated a variety of models for both the oxidized (Fe(III)) and the reduced (Fe(II)) mode of nitrite.

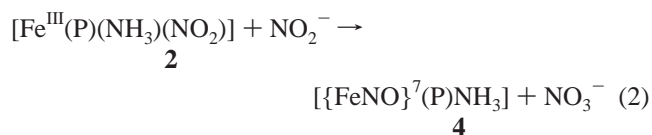
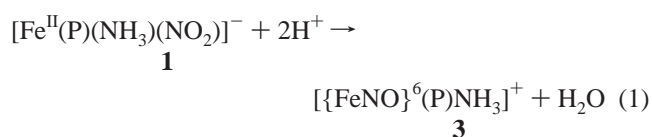
For the oxidized model [Fe(III) (P)(NH₃)(NO₂)] (species **2**), an N-bound structure with a low-spin ($S = 1/2$) configuration was calculated. As expected, the high-spin ($S = 5/2$) state or O-bound structures are energetically unfavorable by more than 10 kcal/mol. This is in agreement with the crystal structure of the substrate nitrite (Figure 2A), which shows binding through the nitrogen atom, with a bond length of 1.9 Å for the Fe–N bond to nitrite. The computed Fe–N bond length of 1.922 Å agrees well with this and also with values obtained from model complexes.^{28–32} For the reduced form [Fe(II) (P)(NH₃)(NO₂)][–] (**1**, Figure 3), an N-bound structure with a low-spin configuration ($S = 0$) was calculated. Again, the predicted Fe–N distance of 1.932 Å is in excellent agreement with the experimental value 1.951 Å for [Fe(II)(TpipPP)(NO₂)(Py)][–],³¹ and the high-spin state ($S = 2$) is higher in energy by ~8 kcal/mol.

Back-Bonding Stabilizes the Enzyme–Substrate Complex. To obtain the iron(III)–nitrite complex structure, nitrite had to be soaked into ccNiR crystals in high excess. This is surprising, as an efficient reductase such as ccNiR should have a high substrate binding constant, and furthermore, the binding of the nitrite anion to Fe(III) should be even more favorable than that to Fe(II) because of the more favorable electrostatic interaction. Interestingly, both spectroscopic³³ and computational studies show the opposite: the reduced form of the active site binds nitrite much more strongly than the oxidized form. For the two models with neutral ligands [Fe(III)(P)(NH₃)(HNO₂)]⁺ and [Fe(II)(P)(NH₃)(HNO₂)]⁰, reaction energies for the exchange of a water ligand against the protonated nitrite molecule are +6.8 and –34.2 kcal/mol, respectively. Here, we followed the practice suggested by Siegbahn to estimate reaction energies preferentially for neutral models, as this yields generally more realistic results.^{8,34}

The explanation for this is a pronounced back-bonding effect which occurs in the Fe(II) form but not in the Fe(III) form, as the iron 3d orbitals are more strongly stabilized because of the increased nuclear charge of the Fe(III) ion relative to the Fe(II) ion. Therefore, the 3d orbitals are *not* available for back-bonding in the oxidized active site but are readily available in the reduced active site (Figure 4A). This back-bonding interaction, which has also been observed in model complexes,³¹ is of fundamental importance for the initial steps of the mechanism, as explained below.

Cleavage of the First N–O Bond. Upon the binding of nitrite to the active site, one of its N–O bonds will break, and this can occur either as a homolytic or as a heterolytic cleavage. Scheidt and co-workers have shown that iron(III)–nitrite adducts are strong O-atom transfer agents, while iron(II)–nitrite adducts react via heterolysis of the N–O bond.^{28,29} Additionally, homolytic cleavages were described as involving a second nitrite molecule to yield nitrate and a {FeNO}⁷ species.³⁵ (In this *Enemark and Feltham notation*, the superscript indicates the number of metal d-electrons plus the number of NO π^* -electrons. This is necessary because the charge distributions in the metal–NO adducts are frequently ambiguous.) However, in the ccNiR system, the active site cavity will not accommodate a second nitrite molecule, and the formation of nitrate is also not detected *in vitro*, even when a high excess of nitrite is present.³⁶

In the two possible reactions



N–O bond heterolysis leads to a {FeNO}⁶ species, (**3**, Figure 3), while homolysis would lead to an {FeNO}⁷ adduct, (**4**, Figure 3). Both reactions were calculated to be energetically possible, but on the basis of the results obtained for the substrate binding step, we strongly favor the heterolytic cleavage of the N–O bond starting from the reduced active site.

The heterolysis of the N–O bond is facilitated by at least two electronic effects. First, the back-bonding interaction transfers charge from the occupied iron-derived t_{2g} -like orbitals into the nitrite π^* orbital (the LUMO of nitrite, Figure 4B). Thus, at the same time, back-bonding leads to an increased strength of the Fe–N bond and, hence, strong binding of the substrate to the reduced active site. Simultaneously, the N–O bond becomes weakened because of the transfer of electron density into an orbital that is antibonding with respect to the N–O bond. This exceptionally strong back-bonding of nitrite with iron(II)–porphyrins is also exemplified by the remarkable fact that even five coordinate iron(II)–nitrite porphyrins show an $S = 0$ low-spin configuration.^{31,32}

The second electronic effect that contributes to the heterolysis of the N–O bond is the formation of hydrogen bonds from protein residues to the oxygens of nitrite. In our structure, the two oxygen atoms of nitrite are in hydrogen bonding distances to the N _{ϵ} atom of His 277 (2.6 Å) and to the N _{ϵ 2} atom of Arg 114 (2.8 Å). To serve as a proton donor, His 277 has to be present in the doubly protonated imidazolium form, which is presumably stabilized by a set of hydrogen bonds between N _{δ} of the same imidazole ring and the backbone carbonyl oxygens of Val 216, Gln 276, and His 277 (Figure 2A). This situation is

(25) Williams, P. A.; Fülöp, V.; Garman, E. F.; Saunders, N. F. W.; Ferguson, S. J.; Hajdu, J. *Nature* **1997**, *389*, 406–412.

(26) Crane, B. R.; Siegel, L. M.; Getzoff, E. D. *Biochemistry* **1997**, *36*, 12120–12137.

(27) Murphy, M. E.; Turley, S.; Adman, E. T. *J. Biol. Chem.* **1997**, *272*, 28455–28460.

(28) Finnegan, M. G.; Lappin, A. G.; Scheidt, W. R. *Inorg. Chem.* **1990**, *29*, 181–185.

(29) Munro, O. Q.; Scheidt, W. R. *Inorg. Chem.* **1998**, *37*, 2308–2316.

(30) Nasri, H.; Ellison, M. K.; Chen, S. X.; Huynh, B. H.; Scheidt, W. R. *J. Am. Chem. Soc.* **1997**, *119*, 6274–6283.

(31) Nasri, H.; Ellison, M. K.; Krebs, C.; Huynh, B. H.; Scheidt, W. R. *J. Am. Chem. Soc.* **2000**, *122*, 10795–10804.

(32) Nasri, H.; Wang, Y.; Huynh, B. H.; Scheidt, W. R. *J. Am. Chem. Soc.* **1991**, *113*, 717–719.

(33) Ranghino, G.; Scorza, E.; Sjögren, T.; Williams, P. A.; Ricci, M.; Hajdu, J. *Biochemistry* **2000**, *39*, 10958–10966.

(34) Siegbahn, P. E. M. *J. Am. Chem. Soc.* **1998**, *120*, 8417–8429.

(35) Enemark, J. H.; Feltham, R. D. *Coord. Chem. Rev.* **1974**, *13*, 339–406.

(36) Stach, P. Dissertation. Mathematisch-Naturwissenschaftliche Sektion, Universität Konstanz, Konstanz, Germany, 2001.

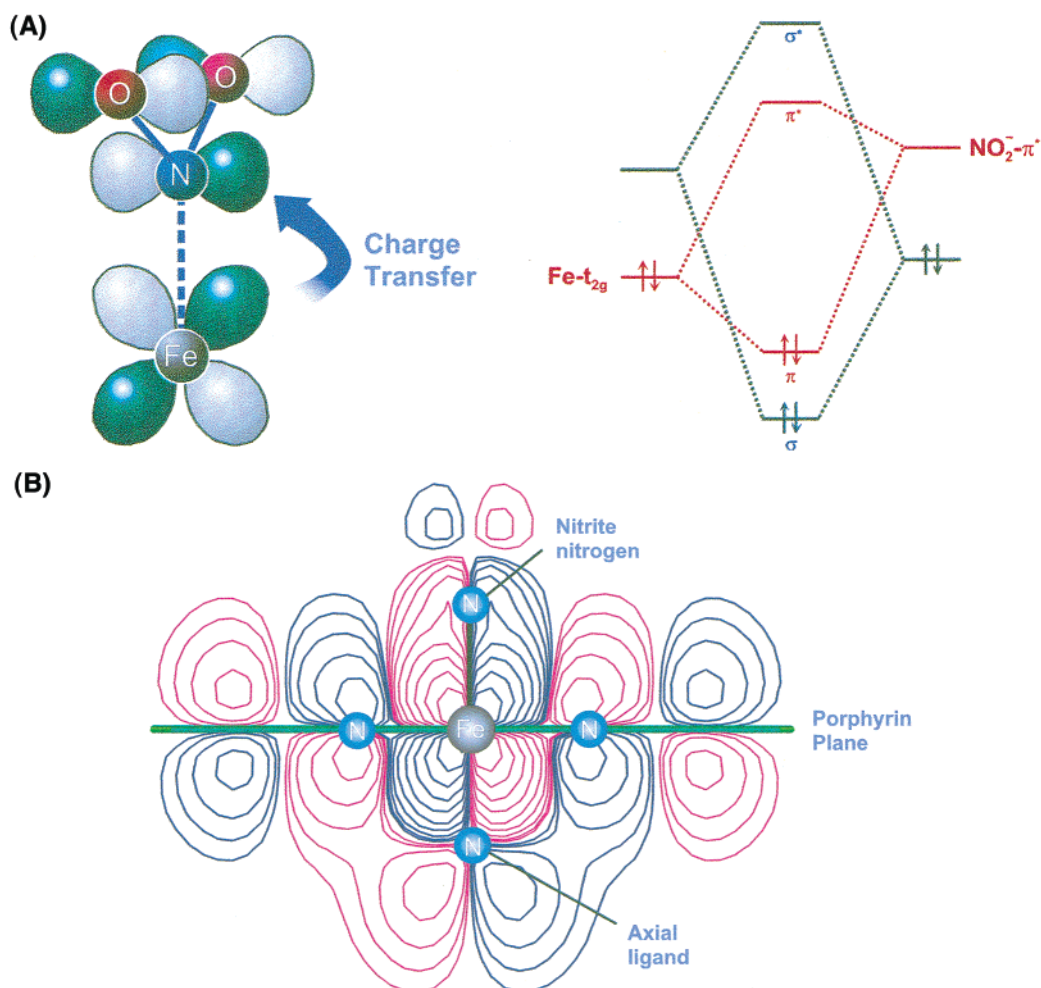


Figure 4. (A) Back-bonding interaction in the porphyrin-nitrite complex transfers charge from the occupied iron-derived t_{2g} -like orbitals into the nitrite π^* orbital. (B) Back-bonding interaction in $[\text{Fe}(\text{II})(\text{P})(\text{NH}_3)(\text{NO}_2^-)]^-$. The contour shows a cut through the iron d_{yz} -based HOMO that has a constructive overlap with the nitrite π^* LUMO, which indicates the back-bonding interaction. The oxygen atoms of nitrite are below and above the plane of the paper, respectively.

reminiscent of the stabilization of the imidazolium ion by an aspartate side chain in the classic serine proteases.³⁷

The electronic effect of the hydrogen bonding is to induce an asymmetry in the two N–O bonds (formal bond order 1.5). Consequently, one of the N–O bonds acquires double bond character, and the other single bond character. Thus, the latter N–O bond is weakened considerably by the presence of H-bonds which should facilitate its cleavage. In addition, the H-bond formation stabilizes the nitrite π^* -orbital, bringing it energetically even closer to the iron 3d-derived orbitals, and thus, the H-bond formation also enhances the back-bonding effect.

In model studies, the binding of nitrite to iron(II)–porphyrins also led to the immediate heterolytic cleavage of an N–O bond and subsequent formation of an Fe(III)–NO ($\{\text{FeNO}\}^6$) species and water.³⁸ Not surprisingly, this step was found to be strongly pH dependent and to occur only below pH 2.7, which presumably reflects the lowered proton affinity of nitrite (the $\text{p}K_a$ of free nitrous acid is ~ 3.4 ³⁹) upon binding to the metal ion. In

the active site of ccNiR, specific provision of protons by the protein can overcome the requirement of the reaction for an unphysiological pH. Because of the arrangement of the protein residues in the active site cavity and from comparing the nitrite complex structure with the hydroxylamine complex (see below), we conclude that the oxygen atom which is hydrogen bonded to His 277 is cleaved first.

Reactivity of the NO Adduct. $\{\text{FeNO}\}^6$ adducts are much less common than their $\{\text{FeNO}\}^7$ counterparts in porphyrin chemistry and are distinctly less stable.^{40–42} The computed structures for the $\{\text{FeNO}\}^6$ and $\{\text{FeNO}\}^7$ forms of the active site may be compared with structurally characterized model complexes.^{42–44} In both cases, excellent agreement between computed and experimental structures is found. Thus, the $\{\text{FeNO}\}^6$ form features a linear Fe–NO unit with a short Fe–N bond of 1.630 Å, while the $\{\text{FeNO}\}^7$ unit is bent with an angle of 139° and an Fe–N bond length of 1.772 Å. In terms of electronic structure, the $\{\text{FeNO}\}^6$ form is best described as a closed-shell species ($S = 0$), with a low-spin Fe(II) ion and a

(37) Matthews, B. W.; Sigler, P. B.; Henderson, R.; Blow, D. M. *Nature* **1967**, *214*, 652–656.

(38) Barley, M. H.; Takeuchi, K. J.; Meyer, T. J. *J. Am. Chem. Soc.* **1986**, *108*, 5876–5885.

(39) Atkins, P. W. *General Chemistry*; Scientific American Books: New York, 1989.

(40) Sharma, V. S.; Traylor, T. G.; Gardiner, R. *Biochemistry* **1987**, *26*, 3837–3843.

(41) Traylor, T. G.; Sharma, V. S. *Biochemistry* **1992**, *31*, 2847–2849.

(42) Ellison, M. K.; Scheidt, W. R. *J. Am. Chem. Soc.* **1997**, *119*, 7404–7405.

(43) Ellison, M. K.; Schulz, C. E.; Scheidt, W. R. *Inorg. Chem.* **2001**, *40*, 1402.

(44) Ellison, M. K.; Schulz, C. E.; Scheidt, W. R. *Inorg. Chem.* **2000**, *39*, 5102–5110.

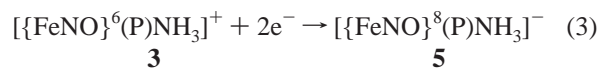
bound NO^+ , which is in agreement with previous suggestions for such species.^{45,46} However, the bending of the coordinated NO-ligand in $\{\text{FeNO}\}^6$ porphyrins is known to be a low-energy motion,⁴⁷ and several significantly bent $\{\text{FeNO}\}^6$ species have been observed in model systems^{48–52} and proteins.^{53–56} Similarly, the $\{\text{FeNO}\}^7$ form is a $S = 1/2$ species with the main contributions to the electronic structure being characterized as Fe(II) bound to NO^* . Traces of this species have been observed under turnover conditions.⁴ For $\{\text{FeNO}\}^7$, our calculations are in good agreement with earlier work⁵⁷ and with more recent theoretical results available in the literature.^{58–60}

Three alternative reactivities can be envisioned for $\{\text{FeNO}\}^6$: (a) protonation of the bound NO^+ , (b) reduction to the $\{\text{FeNO}\}^7$ form, or (c) a coupled proton–electron transfer to yield an HNO species. Since the bound NO^+ should be fairly electrophilic, reaction c was considered to be reasonable. The hydrogen atom for this reaction could be provided by Tyr 217, which is in close contact to the active site (Figure 2A and B) and could form a rather stable tyrosyl radical as an intermediate. However, the calculated energies for a hydrogen atom transfer to either the $\{\text{FeNO}\}^6$ or the $\{\text{FeNO}\}^7$ form yield very positive values (+28.9 and +23.6 kcal/mol, respectively), while at the same time the strength of the tyrosine O–H bond (86 ± 2 kcal/mol⁶¹) is very well reproduced by the present methodology.⁶² Thus, a hydrogen atom transfer from tyrosine to the bound NO^+ is unlikely in this step of the reaction. Protonation of the bound NO^+ is also highly unlikely on the basis of its electrophilic nature and is also not observed in model complexes. Consequently, the most attractive mechanism involves further reduction steps.

Reduction of the $\{\text{FeNO}\}^6$ Species. The $\{\text{FeNO}\}^7$ adduct is known to be highly stable, and although this species can be created *in vitro* by reacting reduced ccNiR with NO, it would probably be a kinetic trap in the reaction of the enzyme *in vivo*. This problem can be overcome if the reduction occurs in two rapid consecutive one-electron reductions to form an $\{\text{FeNO}\}^8$ species (**5**, Figure 3). The rationale for this lies in the fact that, from the $\{\text{FeNO}\}^6$ to the $\{\text{FeNO}\}^7$ adduct, a linear-to-bent transition of the Fe–NO unit has to occur (see earlier). If the transfer of two electrons can be achieved before this chemical

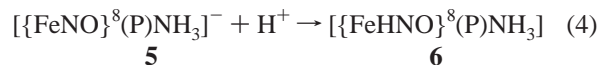
rearrangement takes place, the stable $\{\text{FeNO}\}^7$ form will not play a significant role.

Thus, we propose reaction 3



which involves two one-electron reduction steps that may not be experimentally discernible. The intricate *three*-heme arrangement at the active site of ccNiR might serve the purpose of rapidly injecting a *pair* of electrons into the active site. This would also differentiate ccNiR from *cd*₁ nitrite reductases, which only have a pair of hemes that, in addition, are thought to undergo a ligand exchange reaction in order to prevent the back reaction at the Fe(III)–NO level.^{25,63}

The $\{\text{FeNO}\}^8$ compound (**5**, Figure 3) has, to the best of our knowledge, so far only been observed in nonheme models.⁶⁴ The reduction potential for the one-electron reduction of **4** is certainly rather negative, but recent experimental results for the reduction of the $\{\text{FeNO}\}^7$ species of myoglobin at a potential of –630 mV versus NHE make this a reasonable suggestion.⁶⁵ Even if the reaction were thermodynamically somewhat uphill in ccNiR, it may readily occur if it is coupled to a series of consecutive reactions, at least one of which is significantly exergonic. Importantly, the reduction that leads from **3** to **5** certainly makes the bound NO ligand much more nucleophilic, and its protonation to yield an HNO species (**6**, Figure 3; reaction 4) is a likely scenario.



Such HNO species have been observed in model systems.⁶⁶ In addition, convincing experimental evidence for the formation of such a species in reduced myoglobin–nitrite has recently been reported.⁶⁵ In contrast, an NOH species in which protonation occurred at the oxygen is higher in energy than that in **6** by ~19 kcal/mol, as is expected from the fact that free HNO is much more stable than NOH (the calculated energy difference is ~23 kcal/mol). Thus, protonation at the oxygen can be ruled out.

The calculated structure of **5** shows a closed-shell species with $S = 0$ that is best described as a low-spin Fe(II) ion with a bound NO^- ($S = 0$) ligand. The calculations predict the $S = 0$ and $S = 2$ states in the $\{\text{FeNO}\}^8$ species to be within 2 kcal/mol, which is within the error limits of the employed methodology. We prefer, however, the $S = 0$ state because experimentally an $S = 0$ state was observed in a nonheme iron site.⁶⁴ For the $\{\text{FeHNO}\}^8$ species, the low-spin state is more stable by as much as 17 kcal/mol. The Fe–N distance is increased to 1.79 Å, the N–O distance to 1.21 Å, and the Fe–N–O angle to 126°. All of these changes are consistent with a low-spin Fe(II)– NO^- ($S = 0$) center, although much remains to be learned about the nature of such species in heme as well as in nonheme environments. Note that a closed-shell diamagnetic formulation is also consistent with the experimentally observed diamagne-

- (45) Wade, R. S.; Castro, C. E. *Chem. Res. Toxicol.* **1990**, *3*, 289–291.
 (46) Gwost, D.; Caulton, K. G. *Inorg. Chem.* **1973**, *12*, 2095–2099.
 (47) Vangberg, T.; Bocian, D. F.; Ghosh, A. *J. Biol. Inorg. Chem.* **1997**, *2*, 526–530.
 (48) Scheidt, W. R.; Lee, Y. J.; Geiger, D. K.; Taylor, K.; Hatano, K. *J. Am. Chem. Soc.* **1982**, *104*, 3367–3374.
 (49) Ellison, M. K.; Scheidt, W. R. *J. Am. Chem. Soc.* **1999**, *121*, 5210–5219.
 (50) Ellison, M. K.; Schulz, C. E.; Scheidt, W. R. *Inorg. Chem.* **1999**, *38*, 100–108.
 (51) Richter-Addo, G. B.; Wheeler, R. A.; Hixson, C. A.; Chen, L.; Khan, M. A.; Ellison, M. K.; Schulz, C. E.; Scheidt, W. R. *J. Am. Chem. Soc.* **2001**, *123*, 6314–6326.
 (52) Wyllie, G. R. A.; Scheidt, W. R. *Chem. Rev.* **2002**, *102*, 1067–1090.
 (53) Ding, X. D.; Weichsel, A.; Andersen, J. F.; Shokhireva, T. K.; Balfour, C. A.; Pierik, A.; Averill, B. A.; Montfort, W. R.; Walker, F. A. *J. Am. Chem. Soc.* **1999**, *121*, 128–138.
 (54) Weichsel, A.; Andersen, J. F.; Robert, S. A.; Montfort, W. R. *Nat. Struct. Biol.* **2000**, *7*, 551–554.
 (55) Roberts, S. A.; Weichsel, A.; Qiu, Y.; Shelnut, J. A.; Walker, F. A.; Montfort, W. R. *Biochemistry* **2001**, *40*, 11327–11337.
 (56) Andersen, J. F.; Weichsel, A.; Balfour, C. A.; Champagne, D. E.; Montfort, W. R. *Structure* **1998**, *6*, 1315–1327.
 (57) Olson, L. W.; Schaeper, D.; Lancon, D.; Kadish, K. M. *J. Am. Chem. Soc.* **1982**, *104*, 2042–2044.
 (58) Patchkovskii, S.; Ziegler, T. *Inorg. Chem.* **2000**, *39*, 5354–5364.
 (59) Wondimagegn, T.; Ghosh, A. *J. Am. Chem. Soc.* **2001**, *123*, 5680–5683.
 (60) Rovira, C.; Kunc, K.; Hutter, J.; Ballone, P.; Parinello, M. *Int. J. Quantum Chem.* **1998**, *69*, 31–35.
 (61) Kerr, J. A. *Handbook of Chemistry and Physics*, 77th ed.; Chemical Rubber Company: Cleveland, OH, 1996.
 (62) Blomberg, M. A.; Siegbahn, P. E. M.; Styring, S.; Babcock, G. T.; Akermark, B.; Korall, P. *J. Am. Chem. Soc.* **1997**, *119*, 8285–8282.

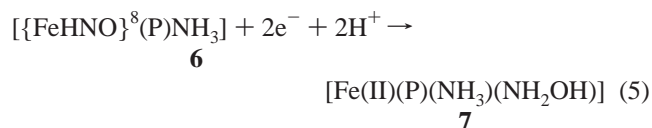
- (63) Allen, J. W. A.; Watmough, N. J.; Ferguson, S. J. *Nat. Struct. Biol.* **2000**, *7*, 885–888.
 (64) Hauser, C.; Glaser, T.; Bill, E.; Weyhermüller, T.; Wieghardt, K. *J. Am. Chem. Soc.* **2000**, *122*, 4352–4365.
 (65) Lin, R.; Farmer, P. J. *J. Am. Chem. Soc.* **2000**, *122*, 2393–2394.
 (66) Bonner, F. T.; Pearsall, K. A. *Inorg. Chem.* **1982**, *21*, 1973–1978.

tism of the $\{\text{FeHNO}\}^8$ species in myoglobin, which allowed its characterization by NMR spectroscopy.⁶⁵

The $\{\text{FeHNO}\}^8$ species also features a closed-shell electronic configuration with a low-spin Fe(II) ion and a neutral, bent HNO ligand. The calculations predict that protonation leaves the Fe–N distance almost invariant but leads to a slight increase in the N–O bond distance to 1.23 Å and a widening of the Fe–N–O angle to 131°. Apart from these changes, the bondings in **5** and **6** appear to be reasonably similar.

In summary, up to this point, it is proposed that the reaction mechanism of ccNiR proceeds through an initial heterolytic cleavage of the N–O bond in **2** to the $\{\text{FeNO}\}^6$ adduct (**4**), which is subsequently reduced in two rapid consecutive one-electron steps to the $\{\text{FeNO}\}^8$ species (**5**), which then becomes protonated to form the $\{\text{FeHNO}\}^8$ species. Note that this part of the reaction happens without changing the valence state of the central iron, which remains in the low-spin Fe(II) state throughout. Since the $\{\text{FeNO}\}^6$ species (**4**) is already best described as Fe(II)–NO⁺, the two reduction steps occur essentially at the NO ligand, and the reason that this is energetically feasible is the low-lying π^* -orbitals on the NO ligand which readily take up two electrons as has previously been discussed by Meyer and co-workers.^{38,67–70}

For the following reduction steps of the HNO adduct, no experimental data are currently available. It appears reasonable to transfer alternately two electrons and two protons to yield an Fe(II) hydroxylamine species (**7**, Figure 3; reaction 5):

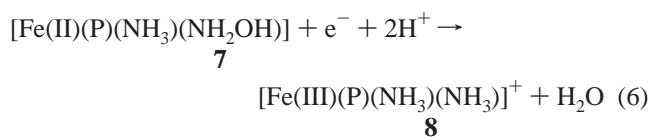


Hydroxylamine as a Reaction Intermediate. The presence of hydroxylamine as an intermediate in the reaction cycle of ccNiR is made plausible by the observation that it is reduced to ammonia by ccNiR with about half the specific activity that is observed for that of nitrite.⁶ By soaking oxidized crystals of ccNiR, we obtained an iron(III)–hydroxylamine complex structure with an end-on bound Fe–NH₂OH unit, in a manner that is fully consistent with the previously observed binding of nitrite (Figure 2B). At the resolution obtained, a distinction between the nitrogen and oxygen atoms of hydroxylamine is not possible, but the binding of the molecule is highly similar to the one of nitrite, with the one oxygen atom missing that was found to interact with His 277 and with a hydrogen bond to the N_ε atom of Arg 114 with a bond length of 3.0 Å. Furthermore, the enzyme was found to reduce *O*-methylated hydroxylamine (methoxyamine).⁶ Unanimously, our calculations show that hydroxylamine should bind via its nitrogen atom to the iron in **7** as well as in the oxidized derivative, Fe(III)–NH₂–OH. We are not aware of structurally characterized model hemes with bound hydroxylamine, but we note a number of complexes

synthesized by Wieghardt and co-workers that show a large structural variability.⁷¹

In the complex structure, the Fe–N bond distance in the hydroxylamine adduct refined to 1.7 Å, but because of the limited resolution of 2.0 Å and the close vicinity of the rather strongly scattering iron atom, this distance must be regarded as less accurate than the one for nitrite determined at a resolution of 1.6 Å. The computed structure for **7** shows that the Fe(II)–NH₂OH bond is fairly normal with a bond length of 2.009 Å, which is slightly shorter than 2.044 Å calculated for that the axial amine ligand. Moreover, the N–O bond also appears to be a fairly normal N–O single bond with a bond length of 1.45 Å. When taken together, this indicates that the metal–ligand bonding in **7** is of the conventional σ -donor type, not unlike those encountered in many complexes with amine nitrogen donors.

Reactivity of the Hydroxylamine Species. By now, the N=O double bond in **4** has been transformed into a single bond in **7** through a series of reduction and protonation steps. It will now be ready for cleavage after injection of a further electron. So far, there is no detailed experimental data available for the reactivity of hydroxylamine bound to Fe(II) heme centers. A single reduction could cleave the N–O bond heterolytically. Oxidation of the Fe(II) ion to Fe(III) coupled to a protonation would then readily yield the product ammonia bound to the Fe(III) form of the active site (**8**, Figure 3; reaction 6):



Iron(III)–porphyrin complexes with NH₃ as a ligand have been reported⁷² but have not been structurally characterized. Structures with ammonia bound to iron(III)–porphyrins have been reported for the protein nitrophorin 4.^{55,56} Experimentally, the complexes show low-spin states with EPR signals of the “large g_{max} ” type,⁷³ and the reported Fe–N distance of 2.05 Å is in good agreement with our calculated distance of 2.013 Å (Table 2). In agreement with the experimental results, the calculations favor a low-spin Fe(III) configuration of the complex. However, the ammonia ligand is not strongly bound, and experimentally, the complexes show a strong tendency to hydrolyze.⁷² The structure calculated for the NH₃ adduct of the Fe(III) active site (**8**) shows a low-spin configuration corresponding to a neutral NH₃ and a low-spin Fe(III) ion. The bond length 2.013 Å appears to be fairly normal for this type of standard σ -donor bond and only changes slightly upon reduction to the Fe(II) form, which is due to the lack of significant π -interactions of the amine nitrogens with the central iron.

Thus, on the basis of the weak binding of ammonia to the Fe(III) form of the active site, the product could readily dissociate and be electrostatically guided to the protein surface through the product channel.^{5,74} The catalytic cycle would be closed by the one-electron reduction of the active site to the Fe(II) form to form species **9** (Figure 3), which could then again

(67) Murphy, W. R.; Takeuchi, K. J.; Meyer, T. J. *J. Am. Chem. Soc.* **1982**, *104*, 5817–5819.

(68) Murphy, W. R.; Takeuchi, K.; Barley, M. H.; Meyer, T. J. *Inorg. Chem.* **1986**, *25*, 1041–1053.

(69) Barley, M. H.; Takeuchi, K.; Murphy, W. R.; Meyer, T. J. *J. Chem. Soc., Chem. Comm.* **1985**, 507–508.

(70) Barley, M. H.; Rhodes, M. R.; Meyer, T. J. *Inorg. Chem.* **1987**, *26*, 1746–1750.

(71) Wieghardt, K. *Adv. Inorg. Bioinorg. Mech.* **1984**, *3*, 213–274.

(72) Kim, Y. O.; Goff, H. M. *Inorg. Chem.* **1990**, *29*, 3907–3908.

(73) Walker, F. A. Personal communication.

(74) Einsle, O.; Stach, P.; Messerschmidt, A.; Klimek, O.; Simon, J.; Kröger, A.; Kroneck, P. M. H. *Acta Crystallogr., Sect. D* **2002**, *58*, 341–342.

bind substrate to initiate the next turnover. Alternatively, it should also be possible for the product to dissociate from the quickly rereduced active site or to be displaced by nitrite. The calculated binding energies for NH_3 of ~ 9 kcal/mol and ~ 14 kcal/mol for the Fe(III) and Fe(II) active sites, respectively, are similar, but a slight favor for dissociation from the Fe(III) state exists.

Reactions 4–6 require protons to enter the reaction mechanism. It is considered likely that these protons derive from the solvent-filled active site cavity, which is accessible through two channels described previously.^{4,5} However, the possibility cannot be excluded that protons are delivered from nearby amino acid side chains.

Conclusion

The proposed mechanism of the six-electron reduction of nitrite to ammonia catalyzed by ccNiR features three essential aspects. The first is that it occurs as a series of reduction and protonation events. Hereby, every reduction is increasing the proton affinity of the substrate or intermediate, and every protonation increases its electrophilicity. This is essential in order to reduce the double bond within the coordinated NO_2^- unit to the point where only a single N–O bond remains, that is, in coordinated NH_2OH . The latter is readily cleaved to give the final product, ammonia. The overall reaction is driven by the continuous supply of electrons along the thermodynamic gradient. The second crucial aspect of the mechanism relates to the spin state of the active site iron. After the binding of nitrite, the system changes from the high-spin to the low-spin potential energy surface. There, the complete reaction can take place, featuring either low-spin Fe(III) ions (t_{2g}^5 configuration) or low-spin Fe(II) ions (t_{2g}^6 configuration). Thus, changes of spin state that would interfere with rapid kinetics are not

required. The third important aspect is the availability of the $\text{NO } \pi^*$ -orbitals to accept two electrons in the early stages of the reaction which significantly contributes to the activation of the second N–O bond.

It is clearly recognized that the six-electron reduction of nitrite to ammonia presents a complicated process which cannot be fully discussed in a single publication. We present a plausible working hypothesis that receives substantial support from both experiments as well as from density functional calculations. The proposed mechanism (Figure 3) is consistent with the currently available experimental data and suggests further experiments which will probe more details of this fascinating multielectron, multiproton-transfer mechanism. In addition, the structural and functional characterizations of suitable low molecular mass model complexes will help to attain a deeper insight and understanding of the reaction mechanism of ccNiR. Ongoing experimental and theoretical work in our laboratories is directed toward an understanding of the role of the lysine axial ligand to the active site. On the basis of preliminary calculations, we do not see any striking electronic reason nature should have chosen an axial lysine over a more conventional histidine ligand.

Acknowledgment. The authors wish to thank Gleb P. Bourenkov and Hans D. Bartunik, MPG-ASMB, DESY Hamburg, for help during synchrotron data collection. This work was supported by Deutsche Forschungsgemeinschaft (F.N., P.K.), German Israeli Foundation (P.K., R.H.), Volkswagenstiftung (P.K.), and Fonds der Chemischen Industrie (F.N., P.K.). The financial contribution to part of the work by EU ERBF MRX-CT98-0204HU (A.M., R.H., O.E.) is acknowledged. We wish to dedicate this work to the memory of Achim Kröger.

JA0206487